Modeling of Camouflage Grass and the Calculation of Its Electromagnetic Scattering Characteristics

WENTAO HE[1], XIAOLONG WENG[1], WEI LUO [1], HAIYAN CHEN[1], XUEYU WU[1], KAI LI[1], YAN HUANG[2], AND BEIPING LIU[2]

[1]National Engineering Research Center of Electromagnetic Radiation Control Materials, Key Laboratory of Multi-spectral Absorbing Materials and Structures of Ministry of Education, School of Electronic Science and Engineering, University of Electronic Science and Technology of China, Chengdu 611731, China
[2]Sichuan Wisepride Industry Company, Ltd., Chengdu 611731, China

Corresponding author: Wei Luo (wei_l@uestc.edu.cn)

ABSTRACT In this work, the complex electromagnetic model of a camouflage grass was accurately generated in geometry, of which the grass leaves were represented by lathy curved rectangular metal surfaces. To investigate the electromagnetic scattering characteristics of the camouflage grass model in the radar band, its radar cross section (RCS) from 4 GHz to 18 GHz was calculated by multilevel fast multipole method (MLFMM). For validation, the camouflage grass sample was manufactured and measured. A relatively good agreement was observed between the results of the calculation and the measurement. Based on this modeling and calculation method, the electromagnetic scattering characteristics of camouflage grass with different leaf lengths, widths, and densities were investigated. According to the numerical results of the application examples, the electromagnetic scattering characteristics changed regularly with the variation of the leaf parameters, and these results were analyzed by electromagnetic wave scattering and phase cancellation. This model will help with the radar camouflage experimental design and electromagnetic scattering investigation of camouflage grass.

INDEX TERMS Camouflage grass, electromagnetic model, calculation, radar cross section, electromagnetic scattering, phase cancellation.

I. INTRODUCTION

With the development of electronic warfare technology, the survivability of modern military targets and the penetration capability of weapon systems are increasingly threatened. Therefore, stealth technology, as an effective means to improve the combat effectiveness of weapons, has attracted extensive attention by many countries worldwide [1]–[4]. The radar stealthy performance of the target is characterized by its radar cross section (RCS) and can be improved by reducing the RCS [5]. There are two main methods for RCS reduction: geometry modification and coating absorbing materials [6], [7]. Geometry modification can reduce the RCS of the target by redirecting the scattered waves away from backscattering directions; however, this method may affect the engineering structural design and the aerodynamics of the targets to some extent. As another important RCS reduction

The associate editor coordinating the review of this manuscript and approving it for publication was Su Yan .

method, traditional coating materials have their own shortcomings, such as a heavy weight, and a poor resistance to high temperature resistance [8]–[10]. Therefore, shielded absorbing materials which possess the advantages of strong absorption, wideband application, light weight, low price, and easy processing has been of increasing interest to scholars and researchers, and many countries pay close attention to this research field.

To the best of our knowledge, there are few studies on shielded absorbing materials that have been reported, among which most have been studies on camouflage net. Few papers presenting researches on camouflage grass have been published. What is more, there are very few investigations on electromagnetic scattering characteristics of grass with bionic design due to its difficult in modeling and complicated calculation [11], [12]. Sasan S. Saatchi et al. investigated microwave backscattering and the emission of grass canopies which consisted of grass, thatch and the underlying soil. In their research, the grass and thatch were modeled by

elongated elliptical discs and a collection of disk shaped water droplets, respectively [13]. James M. Stiles et al. used a numerical solution to solve the scattering problem of cylinders with arbitrary cross sections and investigated a long, thin grass blade structure [14]. Based on these studies they modeled the long, thin elements of the grass canopy as linear dipole elements, and they presented a formulation to describe the microwave scattering from a grassland canopy whose physical structure was accurately considered [15]. Giovanni Macelloni et al. demonstrated the relationship between the backscattering coefficient and the vegetation biomass, and concluded that backscattering became stronger with the increase in broad leaf crop biomass, for which scattering was dominant; in contrast, for narrow-leaf plants, the trend was flat or decreasing because of a major contribution of absorption [16]. Andrea Della Vecchia et al. described the electromagnetic model of crops whose leaves were represented by curved rectangular dielectric surfaces. Theoretical simulations of backscattering from wheat and corn canopies were shown and compared in their paper [17]. Y. Oh et al. presented an examination of classical scattering models for radar cross sections of deciduous leaves, and they concluded that both the physical optics (PO) and generalized Rayleigh-Gans (GRG) models could be used for calculating the scattering matrices of natural deciduous leaves at microwave frequencies [18]. Xueyang Duan et al. developed an electromagnetic scattering model to analyze radar scattering from marsh grass, and they studied the sensitivity of radar observations to the density, structure, and dead-live status of the marsh [19].

In the references mentioned above, several different modeling methods of vegetation were proposed to investigate their electromagnetic scattering properties. However, because of the structural complexity of the bionic vegetation model, hardly any of these studies consider the precise modeling and accurate calculation of the vegetation. Based on these vegetation investigation methods, camouflage grass, a kind of shielded absorbing material, was accurately modeled in geometry and its electromagnetic scattering characteristics were calculated precisely and analyzed in this paper. The camouflage grass leaf was modeled by a lathy curved rectangular metal surface, and the bionic grass structure was obtained by distributing the metal surfaces on a hexagonal array substrate. The major challenges to modeling and calculating the camouflage grass include how to ensure the randomness and authenticity of the extremely large number of grass leaves and how to ensure the feasibility and veracity of the calculation methods for a particularly complicated electromagnetic model with quite a few elaborate and complex structures. To address these problems, the growth conditions of grass in nature were previously investigated, and the ranges of grass leaf length, width, thickness, pitching angle, orientation, and density were determined. Based on these survey data, the camouflage grass was modeled by a random number generator and the operation of permutation and combination. For a complex model such as grass with a large number of elaborate structures, it is quite difficult to solve using an

accurate method because of the large number of unknowns and poor convergence. Considering that the thickness of the grass leaf was approximately dozens of microns, the effect of the thickness can be almost ignored in the radar band. Therefore, the grass leaf was modeled by a metal surface without thickness to reduce the number of unknowns, and a metal plate of the same size was placed under the camouflage grass to improve the convergence.

The rest of this paper is organized as follows: The modeling approach of camouflage grass is described in more detail in Section 2. The monostatic RCS of the camouflage grass was calculated with MLFMM. To verify the reliability of the modeling and calculation method, the camouflage grass sample was prepared, and its monostatic RCS was measured. The comparison results are presented and analyzed in Section 3. In Section 4, the monostatic RCS of camouflage grass models with various leaf lengths, widths, and densities were calculated to investigate their effect on electromagnetic scattering. Finally, some conclusions are given and presented in Section 5.

II. GUIDELINES FOR MANUSCRIPT PREPARATION

To model the camouflage grass, a parabolic function $x = ay^2$ ($a > 0, y \geq 0$) was defined in the Cartesian coordinates system (as shown in Fig. 1), for which '*x*' and '*y*' represent the variables on the *x-axis* and *y-axis*, respectively. The variable '*a*' is the coefficient of the parabola, and 11 different parabolas were generated through adjusting the values of *a*. By adjusting the value range of *y*, the 11 different parabolas obtained the same length of 1.5 cm. In this paper, the angle between the *x* positive axis and the line between the coordinate points where the parabola takes the minimum value and the maximum value was defined as pitching angle α (as shown in Fig. 1), and 11 different pitching angles (25°, 36°, 48°, 55°, 57°, 61°, 65°, 68°, 73°, 77°, 82°) were chosen to determine the pitch degrees of the parabolas.
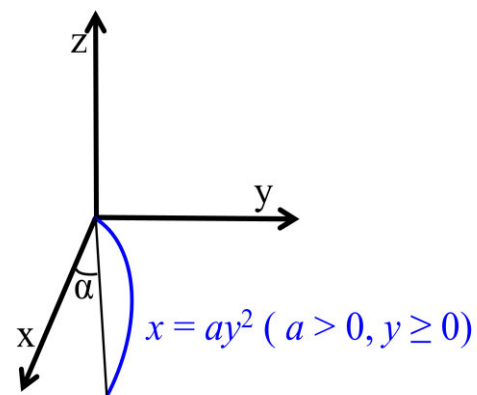

FIGURE 1. Pitching angle α of the parabola $x = ay^2$ ($a > 0, y \geq 0$) in the Cartesian coordinate system.

Then the parabolas were swept to shape curved surfaces with a common width of 1.7 mm, and the curvatures of the curved surfaces were locally adjusted slightly to generate
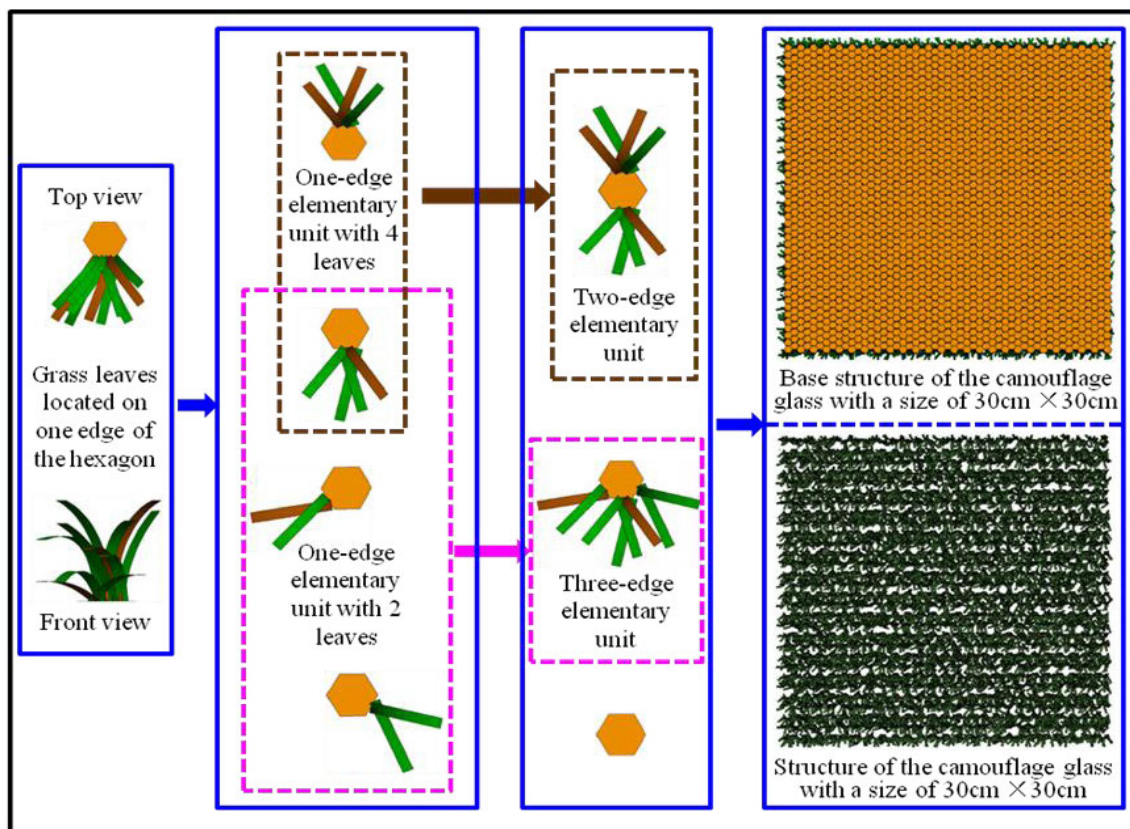
FIGURE 2. Modeling scheme of the camouflage grass with a size of 30 cm × 30 cm.

grass leaves. It is worth mentioning that camouflage grass leaves can be designed with different lengths and widths according to need. However, to prepare camouflage grass samples for comparison and verification, grass leaves were generated with a common length and a common width to simplify the preparation process of the sample.

As shown in Fig. 2, to generate the elementary unit of the camouflage grass, a regular hexagon with a side length of 4 mm was chosen as the base structure. On one edge of the hexagon, 11 equidistant points were obtained by taking a point every 0.4 mm. Then, 11 grass leaves were randomly generated at the positions of the equidistant points. The orientations of the grass leaves were determined by rotating the leaves with random angles which were generated by a random number generator. To adjust the density of the grass leaves, 7 leaves were deleted randomly. Hereto, a one-edge elementary unit with only 4 leaves was obtained. By repeating the delete operation, several different one-edge elementary units could be obtained. Similarly, a three-edge elementary unit with 2 leaves, 4 leaves, and 2 leaves on three adjacent edges of the regular hexagon separately could also be obtained. Likewise, different three-edge elementary units could be generated by delete operation as described in the model process of the one-edge elementary unit.

Based on the method presented above, 256 different one-edge elementary units and 512 different three-edge elementary units were generated in this paper. Then, every two one-edge elementary units were combined to generate 256 different two-edge elementary units. Following the principle of alternative distribution, the two-edge elementary units and three-edge elementary units were randomly arranged into columns. Finally, these columns were distributed with regular hexagons interweaving among them to form a grass structure with all regular hexagons closely arranged in the base structure. The camouflage grass we designed was obtained by deleting the base structure. The dimensions of the camouflage grass can be controlled by adjusting the columns generated by the random arrangement of one-edge elementary units and three-edge elementary units. In this paper, a camouflage grass with dimensions of 30 cm × 30 cm was modeled. Moreover, to avoid generating overlapping mesh triangles, the grass model was simplified to remove overlapping and reduplicative surfaces.

III. MODEL VERIFICATION
Based on the camouflage grass model built above, the monostatic RCS of the model from 4 GHz to 18 GHz was calculated by MLFMM to investigate its electromagnetic scattering characteristics in a wideband. To improve the calculation convergence of the camouflage grass model, a metal plate with a thickness of 0.3 mm and a size of 30 cm × 30 cm was developed under the camouflage grass model
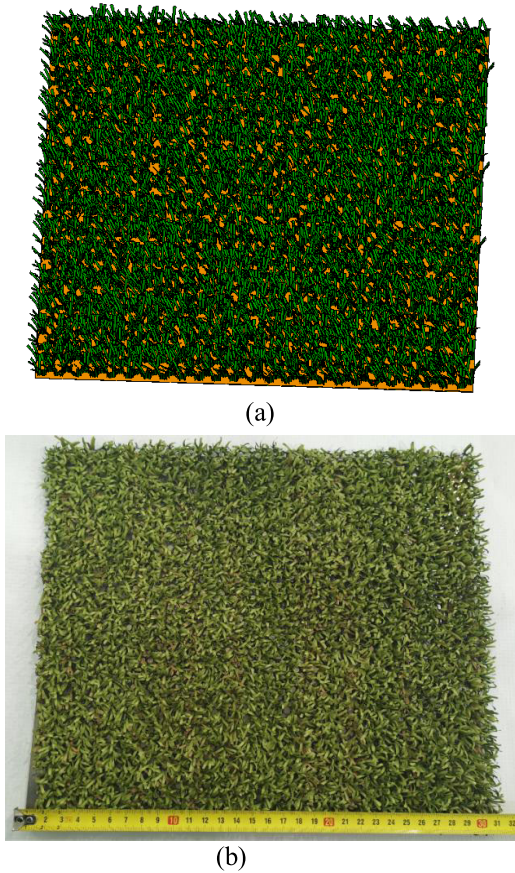
(a)

(b)

FIGURE 3. The camouflage grass with a metal plate under it: (a) calculation model (b) measurement sample.
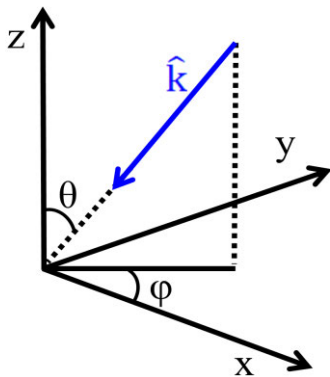

FIGURE 4. Pitching angle θ and azimuth angle φ of the incident electromagnetic wave in the Cartesian coordinate system.

to calculate together (as shown in Fig. 3). Assuming $\hat{k} = -(\hat{x}\sin\theta\cos\varphi + \hat{y}\sin\theta\sin\varphi + \hat{z}\cos\theta)$ is the incident direction of the incident electromagnetic wave (as shown in Fig. 4), then the angle between $\hat{k}$ and the positive z- axis represents the pitching angle θ, and the angle between $\hat{k}$ and the positive x-axis represents the azimuth angle φ. The incident electromagnetic wave was fixed at the pitching angle of $\theta = 0°$ and the azimuth angle of $\varphi = 0°$. The polarization mode of the

incident electromagnetic wave was defined according to the relationship of the electric field direction and coordinate axis. The electric field directions of the incident electromagnetic wave parallel to x-axis and y- axis were defined as HH polarization and VV polarization, respectively. The number of unknowns for the calculated model was 296627, the peak memory requirement was 36.4 GB, and it took 42.6 h to obtain the monostatic RCS values for 281 frequencies.
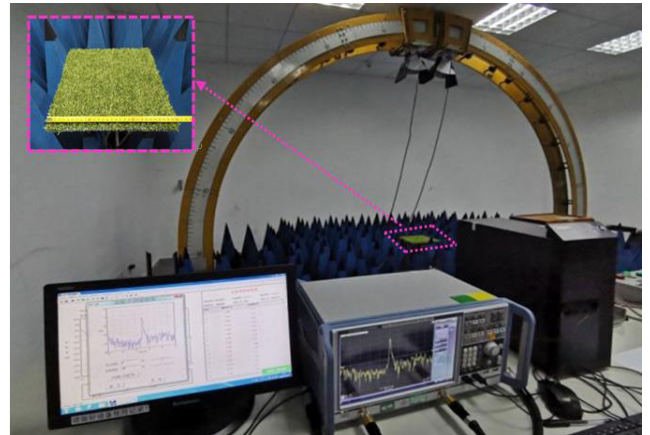

FIGURE 5. The camouflage grass sample measured in the far field range.

To verify the reliability and accuracy of the modeling and calculation methods described above, a camouflage grass sample with the same size as the calculation model was manufactured for measurement. The difference between the calculation model and the measurement sample was that the former ignored the thickness of the grass leaf while the latter had a leaf thickness of 40 μm. As shown in Fig. 5, the camouflage grass sample was measured in a far field range. The measurement system consists of absorbing foams and two horn antennas in which the transmitting antenna illuminates the camouflage grass, and the reflected wave is collected by the receiving antenna. The antennas are placed along the arch according to the incidence angle ($\theta_i = \theta_r$), and the camouflage grass is placed at the center of the arch [20].

Fig. 6 demonstrates the monostatic RCS curves of the camouflage grass obtained by calculation and measurement for HH polarization and VV polarization. By comparing the data, it can be seen that the calculation results agree well with that of the measurement, which indicates that the modeling and analytical method proposed in this work is valid.

However, there were some distinct differences between the calculation curves and measurement curves. This difference was because the randomness of the camouflage grass leaves could not be duplicated by manufacturing, that is, the calculation model differed with the measurement sample to some extent. Even so, the calculation curves matched the measurement curves well in terms of their trends. This result demonstrates that the modeling and calculation methods work for investigating the electromagnetic scattering characteristics of camouflage grass.
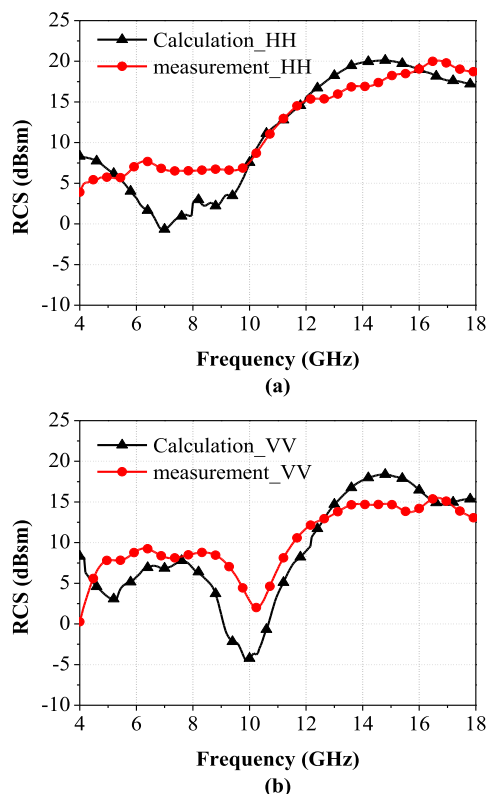
FIGURE 6. The monostatic RCS results of camouflage grass by calculated and measured: (a) HH polarization, (b) VV polarization.

FIGURE 7. The local structures of camouflage grass with different leaf widths.

IV. APPLICATION EXAMPLES

In this section, 3 examples were considered to analyze the influence of leaf parameter variation on the electromagnetic scattering of camouflage grass. With the modeling and calculation methods described above, electromagnetic models with different leaf widths, lengths, and densities were generated. The monostatic RCSs of the camouflage grass models were calculated and analyzed.

The camouflage grass models in the case of different grass leaf widths were first investigated. In this work, three values for the grass leaf width: $W_1 = 1.5$ mm, $W_2 = 1.7$ mm, and $W_3 = 1.9$ mm were chosen as variables. The corresponding grass models were developed and their local structures are presented in Fig. 7 for comparison.

Simultaneously, the camouflage grass models were calculated with MLFMM under the same settings described in Section III. The monostatic RCS curves displayed regular variation with the change of grass leaf width. According to Fig. 8, the RCS curves showed almost no change as the grass leaf width increased in the C-band; However, in the X-band and Ku-band the curves decreased gradually with the increase of grass leaf width, even though the decrease was not very obvious.

The slight change in the monostatic RCS values was due to the scattering and phase cancellation of the electromagnetic waves. When the camouflage grass leaf width gradually increased, the total area of the camouflage grass
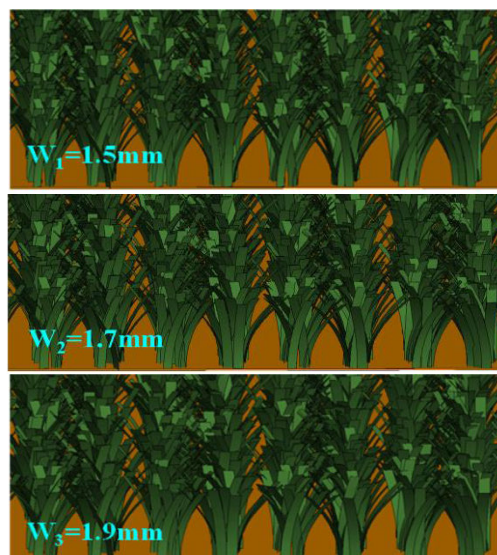
leaf increased, the scattering of the electromagnetic wave occurred more times and the phase cancellation was more complex, which led to a weakening of the echo. Therefore, the camouflage grass with wider leaves had weaker backscattering, that is to say, the monostatic RCS had smaller values.

Then, the influence of the grass leaf length on the electromagnetic scattering characteristics of the camouflage grass was analyzed. As shown in Fig. 9, the leaf length was modeled with $L_1 = 1.0$ cm, $L_2 = 1.5$ cm, and $L_3 = 2.0$ cm for the three different camouflage models. Their monostatic RCSs were calculated and are presented in Fig. 10. The monostatic RCS decreases with the increase of the leaf length. This change can be explained according to the camouflage grass model structure.

From Fig. 10, the camouflage grass leaf with a length of $L_1 = 1.0$ cm results in more exposure of the underlying metal plate. Therefore, the direct scattering from the exposed metal plate, which contributes to the total backscattering can not be ignored [21]. With the increase of the grass leaf length, the metal plate was exposed less and less, which led to a smaller contribution from the metal plate. Therefore, camouflage grass with a longer leaf length corresponded to lower monostatic RCS values. However, for VV polarization, camouflage grass with a leaf length of $L_3 = 2.0$ cm demonstrated anomalous changes in the X-band. A detailed investigation of this phenomenon is beyond the scope of this paper. The scattering mechanism will be explored in our future work.

Finally, the density factor was considered with a defined parameter element unit area index (EUAI). In this manuscript, the unit was composed of a regular hexagon base and some leaves and was called the elementary unit. The regular hexagonal area of the elementary unit was called the elementary unit base area. Then, the ratio of the elementary unit base area to the total camouflage grass base area could be defined as EUAI. According to this definition, three camouflage grass
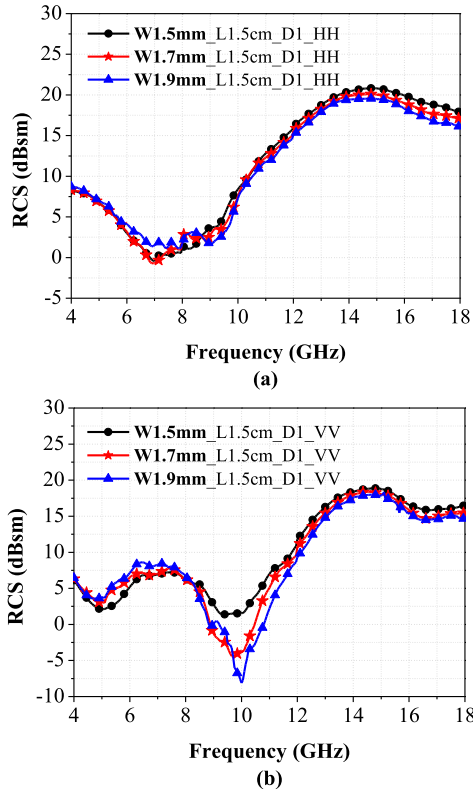
FIGURE 8. The calculated monostatic RCS of camouflage grass with different leaf widths: (a) HH polarization (b) VV polarization.
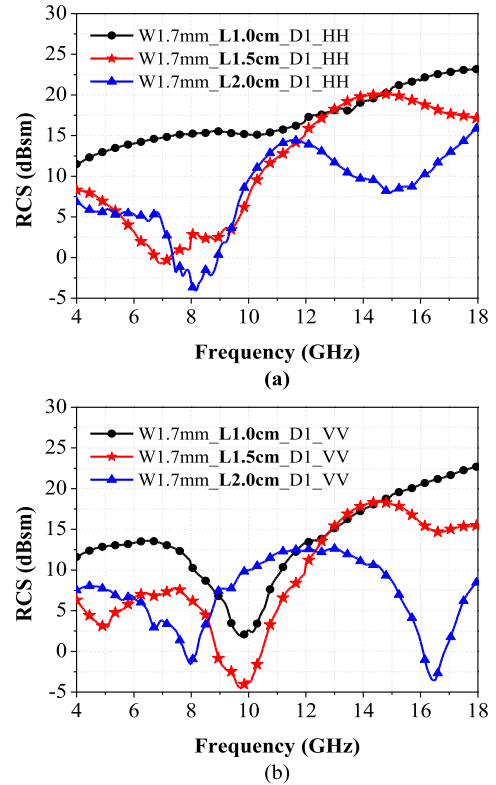

FIGURE 9. The local structures of camouflage grass with different leaf lengths.

FIGURE 10. The calculated monostatic RCS of camouflage grass with different leaf lengths: (a) HH polarization (b) VV polarization.
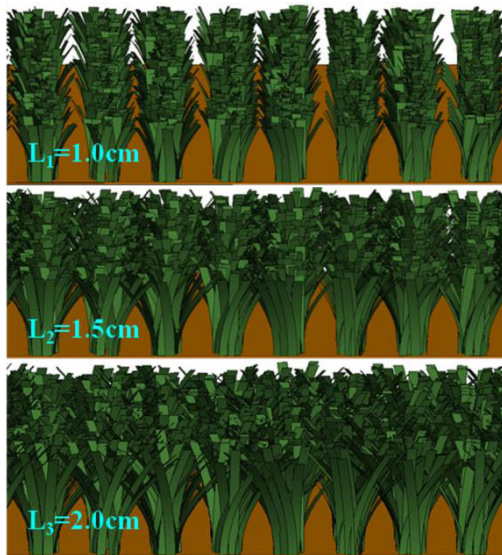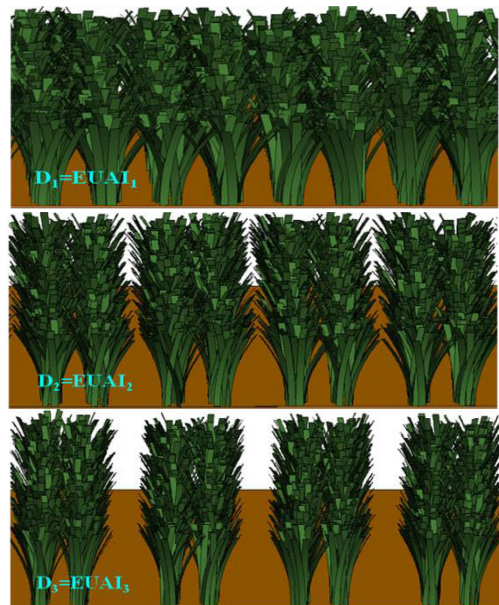

FIGURE 11. The local structures of camouflage grass with different leaf densities.

models with densities of $EUAI_1 = 50\%$, $EUAI_2 = 37.5\%$, and $EUAI_3 = 30\%$ are presented in Fig. 11. The calculated results shown in Fig. 12 demonstrate that the monostatic RCS increases with decreasing camouflage grass density. This phenomenon can be explained by phase cancellation of the electromagnetic waves. The repetitious refraction and

reflection of the incident electromagnetic wave occurred on every curved rectangular metal sheet, leading to phase cancellation of the scattering echoes, which results in a weak total radar echo. The denser the camouflage grass is, the weaker the total radar echoes are [16]. Therefore, the camouflage grass
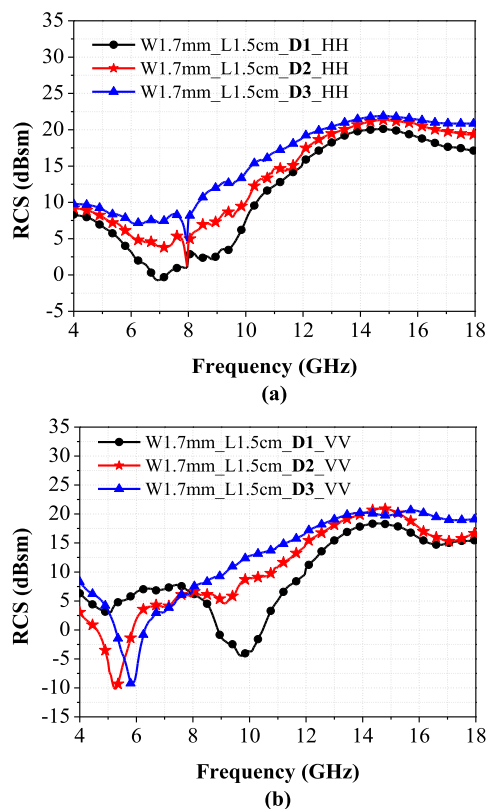
FIGURE 12. The calculated monostatic RCS of camouflage grass with different leaf densities: (a) HH polarization (b) VV polarization.

with a higher EUAI has lower monostatic RCS values. Nevertheless, the curves present different changes in the C-band, which may be because the precision of the calculation is not good enough for elaborate and complex structures at low frequencies.

Due to space limitations, only the 3 parameters described above were considered to investigate their influence on the electromagnetic scattering of camouflage grass. There are still other factors that may need to be considered, such as the pitching angle of the grass leaf, and the ups and downs of the camouflage grass. A further investigation including these problems will be presented in our future work.

V. CONCLUSION

A camouflage grass model with complicated and elaborate structures was accurately designed and built in geometry. The MLFMM was used to calculate its electromagnetic scattering properties by modeling a metal plate with the same size under its base structure to improve the convergence. For comparison and verification, the camouflage grass sample was manufactured and measured under the same conditions. The calculation and measurement of monostatic RCS curves were compared from 4 GHz to 18 GHz, and the relatively good agreement between them demonstrated the reliability and accuracy of our modeling and calculation methods. Moreover, the influence of grass width, grass length, and grass

density on the electromagnetic scattering characteristics of camouflage grass was investigated. The calculation results were presented and analyzed.

As the model results show in this paper, electromagnetic scattering from camouflage grass is extremely complicated and easily affected by different parameters. The relationships can be established from the calculation results: the grass width variation does not change much in the backscattering of the camouflage grass. However, as the grass length increases, the backscattering of the camouflage grass obviously weakens, and the same relationship can be observed between the grass density and the backscattering.

REFERENCES

[1] C.-Y. Wang, J.-G. Liang, T. Cai, H.-P. Li, W.-Y. Ji, Q. Zhang, and C.-W. Zhang, "High-performance and ultra-broadband metamaterial absorber based on mixed absorption mechanisms," *IEEE Access*, vol. 7, pp. 57259–57266, 2019.

[2] Y. Zhuang, G. Wang, Q. Zhang, and C. Zhou, "Low-scattering tri-band metasurface using combination of diffusion, absorption and cancellation," *IEEE Access*, vol. 6, pp. 17306–17312, 2018.

[3] Z. Liu, Y. Liu, and S. Gong, "Gain enhanced circularly polarized antenna with RCS reduction based on metasurface," *IEEE Access*, vol. 6, pp. 46856–46862, 2018.

[4] H. Zeng, X. Zhao, Q. Su, Y. Zhang, and H. Li, "Fast coating analysis and modeling for RCS reduction of aircraft," *Chin. J. Aeronaut.*, vol. 32, no. 6, pp. 1481–1487, Jun. 2019.

[5] L. Yuan, B. Wang, W. Gao, Y. Xu, X. Wang, and Q. Wu, "An effective methodology to design scale model for magnetic absorbing coatings based on ORL," *Results Phys.*, vol. 7, pp. 1698–1704, Jan. 2017.

[6] J. Song, X. Wu, C. Huang, J. Yang, C. Ji, C. Zhang, and X. Luo, "Broadband and tunable RCS reduction using high-order reflections and salisbury-type absorption mechanisms," *Sci. Rep.*, vol. 9, no. 1, Jun. 2019, Art. no. 9036.

[7] J. Cui and Y. Yang, "Visual computing of complicated target with radar absorbing material," *Chin. J. Electron.*, vol. 25, no. 1, pp. 106–113, Jan. 2016.

[8] H. B. Baskey, E. Johari, and M. J. Akhtar, "Metamaterial structure integrated with a dielectric absorber for wideband reduction of antennas radar cross section," *IEEE Trans. Electromagn. Compat.*, vol. 59, no. 4, pp. 1060–1069, Aug. 2017.

[9] Y.-C. Hou, W.-J. Liao, J.-F. Ke, and Z.-C. Zhang, "Broadband and broad-angle dielectric-loaded RCS reduction structures," *IEEE Trans. Antennas Propag.*, vol. 67, no. 5, pp. 3334–3345, May 2019.

[10] G.-S. Bae and C. Y. Kim, "Broadband multilayer radar absorbing coating for RCS reduction," *Microw. Opt. Technol. Lett.*, vol. 56, no. 8, pp. 1907–1910, May 2014.

[11] Y. Yang, W. Luo, B. Yin, and Y. Ren, "Electromagnetic scattering of rough ground surface covered by multilayers vegetation," *Int. J. Antennas Propag.*, vol. 2019, Apr. 2019, Art. no. 9413058, doi: 10.1155/2019/9413058.

[12] C. Yang and Y. Du, "Characterization of ICA for scattering from cylindrical components of vegetation," *IEEE Geosci. Remote Sens. Lett.*, vol. 15, no. 12, pp. 1902–1906, Dec. 2018.

[13] S. S. Saatchi, D. M. Le Vine, and R. H. Lang, "Microwave backscattering and emission model for grass canopies," *IEEE Trans. Geosci. Remote Sens.*, vol. 32, no. 1, pp. 177–186, Jan. 1994.

[14] J. M. Stiles, K. Sarabandi, and F. T. Ulaby, "Microwave scattering model for grass blade structures," *IEEE Trans. Geosci. Remote Sens.*, vol. 31, no. 5, pp. 1051–1059, Sep. 1993.

[15] J. M. Stiles and K. Sarabandi, "Electromagnetic scattering from grassland. I. a fully phase-coherent scattering model," *IEEE Trans. Geosci. Remote Sens.*, vol. 38, no. 1, pp. 339–348, Jan. 2000.

[16] G. Macelloni, S. Paloscia, P. Pampaloni, F. Marliani, and M. Gai, "The relationship between the backscattering coefficient and the biomass of narrow and broad leaf crops," *IEEE Trans. Geosci. Remote Sens.*, vol. 39, no. 4, pp. 873–884, Apr. 2001.

[17] A. D. Vecchia, P. Ferrazzoli, and L. Guerriero, "Modelling microwave scattering from long curved leaves," *Waves Random Media*, vol. 14, no. 2, pp. S333–S343, Apr. 2004.

[18] Y. Oh and J.-Y. Hong, "Re-examination of analytical models for microwave scattering from deciduous leaves," *IET Microw., Antennas Propag.*, vol. 1, no. 3, pp. 617–623, 2007.

[19] L. Liu, Y. Shao, N. Pinel, K. Li, Z. Yang, H. Gong, and Y. Wang, "Modeling microwave backscattering from parabolic rice leaves," *IEEE Trans. Geosci. Remote Sens.*, vol. 55, no. 11, pp. 6044–6053, Nov. 2017.

[20] H. Chen, R. Shen, F. Li, Y. Zhou, L. Zhang, X. Weng, H. Lu, J. Xie, and L. Deng, "Design of phase matching chessboard–like electromagnetic metasurfaces for wideband radar cross section reduction," *Microw. Opt. Technol. Lett.*, vol. 61, no. 9, pp. 2037–2045, Apr. 2019.

[21] X. Duan and C. E. Jones, "Coherent microwave scattering model of marsh grass," *Radio Sci.*, vol. 52, no. 12, pp. 1578–1595, Dec. 2017.
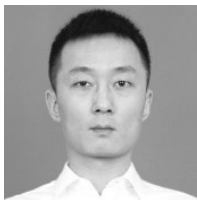
WENTAO HE was born in Xuchang, China. He received the B.S. degree in materials physics from the Nanjing University of Posts and Telecommunications, Nanjing, China, in 2014. He is currently pursuing the Ph.D. degree in materials science and engineering with the University of Electronic Science and Technology of China, Chengdu, China.

His research interests include computational electromagnetic, RCS reduction, structure design of targets for radar stealth, and the electromagnetic scattering of typical targets in a complex ground environment.

XIAOLONG WENG received the B.S. degree in polymer materials from the North China Institute of Technology, Taiyuan, China, in 1995, and the M.S. degree in applied chemistry from the Logistical Engineering College of the People's Liberation Army of China, Chongqing, China, in 2002.

He is currently a Professor with the University of Electronic Science and Technology of China, Chengdu, China. He has authored or coauthored over ten journal papers. His research interests include infrared stealth materials, multispectrum stealth materials, and intelligent materials.
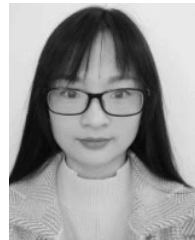
WEI LUO received the B.S. degree in materials science from Zhejiang University, Hangzhou, China, in 1993, and the Ph.D. degree in materials physics and chemistry from the University of Electronic Science and Technology of China, Chengdu, China, in 2007.

He is currently an University Lecturer with the University of Electronic Science and Technology of China. His research interests include electromagnetic scattering calculation and fast algorithms, RCS reduction, and the mechanism of interaction between magnetic materials and electromagnetic waves and fields.
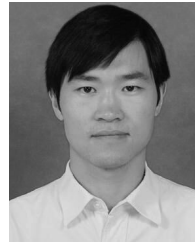
HAIYAN CHEN received the B.S. degree in chemical machinery from Sichuan University, Chengdu, China, in 1999, the M.S. degree in microelectronics and solid electronics from the Chongqing University of Posts and Telecommunications, Chongqing, China, in 2006, and the Ph.D. degree in microelectronics and solid-state electronics from the University of Electronic Science and Technology of China, Chengdu, in 2011.

He is currently an Associate Professor with the University of Electronic Science and Technology of China. His research interests include artificial electromagnetic materials, electromagnetic radiation control materials, and particularly studies on electromagnetic discontinuous repair materials.

XUEYU WU received the B.S. degree in materials science and engineering from the Southwest University of Science and Technology, Mianyang, China, in 2015. She is currently pursuing the Ph.D. degree in materials science and engineering with the University of Electronic Science and Technology of China, Chengdu, China.

Her research interests include intelligent thermal control of spacecraft and infrared stealth material, and the selective absorption mechanism of phase change materials with different structures.

KAI LI was born in Weifang, Shandong, China, in 1994. He received the B.S. degree from the Qingdao University of Science and Technology, Qiangdao, China, in 2017. He is currently pursuing the M.S. degree with the University of Electronic Science and Technology of China, Chengdu, China.

His main research interests include the metamaterial absorbing structure and RCS reduction.

YAN HUANG received the B.S. degree in polymer materials and engineering from Southwest Petroleum University, Chengdu, China, in 2014.

She is currently working with Sichuan Wisepride Industry Company, Ltd., Chengdu, China. Her main works include electromagnetic simulation, RCS reduction and stealth optimization, and camouflage pattern design.

BEIPING LIU received the B.S. degree in applied chemistry from the Southwest University of Science and Technology, Mianyang, China, in 2009.

He is currently working with Sichuan Wisepride Industry Company, Ltd., Chengdu, China. His main works include materials research of camouflage grass, technology development, equipment development, and products manufacturing.

• • •